HHS Public Access

Author manuscript

Oncogene. Author manuscript; available in PMC 2015 April 02.

Published in final edited form as:

Oncogene. 2014 October 2; 33(40): 4867–4876. doi:10.1038/onc.2013.439.

HSP-90 Inhibitor Ganetespib is Synergistic with Doxorubicin in Small Cell Lung Cancer

Chien-Hao Lai[1,4], **Kang-Seo Park**[1], **Dae-Hao Lee**[1], **Anna Teresa Alberobello**[1], **Mark Raffeld**[2], **Mariaelena Pierobon**[3], **Elisa Pin**[3], **Emanuel F. Petricoin III**[3], **Yisong Wang**[1,*], and **Giuseppe Giaccone**[1,*]

[1]Medical Oncology Branch, National Cancer Institute, National Institutes of Health, Bethesda, Maryland, United States

[2]Laboratory of Pathology, National Cancer Institute, National Institutes of Health, Bethesda, Maryland, United States

[3]Center for Applied Proteomics and Molecular Medicine, George Masson University, Manassas, Virginia 20110, United States

Abstract

SCLC at advanced stage is considered an incurable disease. Despite good response to initial chemotherapy, the responses in SCLC patients with metastatic disease are of short duration and resistance inevitably occurs. Although several target-specific drugs have altered the paradigm of treatment for many other cancers, we have yet to witness a revolution of the same magnitude in SCLC treatment. Anthracyclines, such as doxorubicin, have definite activity in this disease, and ganetespib has shown promising activity in preclinical models, but underwhelming activity as a single agent in SCLC patients. Using SCLC cell lines, we demonstrated that ganetespib (IC50: 31nM) was much more potent than 17-AAG, a geldanamycin derivative (IC50: 16 μM). Ganetespib inhibited SCLC cell growth via induction of persistent G2/M arrest and Caspase 3-dependent cell death. MTS assay revealed that ganetespib synergized with both doxorubicin and etoposide, two topoisomerase II inhibitors commonly used in SCLC chemotherapy. Expression of RIP1, a protein that may function as a pro-survival scaffold protein or a pro-death kinase in TNFR1-activated cells, was induced by doxorubicin and downregulated by ganetespib. Depletion of RIP1 by either RIP1 siRNA or ganetespib sensitized doxorubicin-induced cell death, suggesting that RIP1 may promote survival in doxorubicin-treated cells and that ganetespib may synergize with doxorubicin in part through downregulation of RIP1. In comparison to ganetespib or doxorubicin alone, the ganetespib + doxorubicin combination caused significantly more growth regression and death of human SCLC xenografts in immuocompromised mice. We conclude that genetespib and doxorubicin combination exhibits significant synergy and is efficacious in

Corresponding Authors: Giuseppe Giaccone and Yisong Wang, Lombardi Comprehensive Cancer Center, Georgetown University, 3970 Reservoir Road, Washington DC 20007, tel 202 6877072, fax 202 6870313, gg496@georgetown.edu and yw350@georgetown.edu.

[4]Current Institution: Division of Pulmonary and Critical Care Medicine, Department of Internal Medicine, Kaohsiung Chang Gung Memorial Hospital, Chang Gung University College of Medicine, Kaohsiung, Taiwan

Conflict of Interest: The authors have no conflict of interest to disclose.

inhibiting SCLC growth in vitro and in mouse xenograft models. Our preclinical study suggests that ganetespib and doxorubicin combination therapy may be an effective strategy for SCLC treatment, which warrants clinical testing.

Keywords

Doxorubicin; Ganetespib; HSP90 inhibitor; RIP1; SCLC

Introduction

Small cell lung cancer (SCLC) is an aggressive form of lung cancer accounting for about 10–20% of pulmonary malignancies, strongly associated with cigarette smoking, poor survival rates, and early metastatic spreading [1, 2]. Operation is seldom performed and chemotherapy coupled with chest radiotherapy in cases limited to the chest is the mainstay of treatment for this disease. Although chemotherapy has high response rates of over 50%, median survival of SCLC is only approximately 10–12 months for patients with extensive disease and 18–24 months for patients with limited disease [1–3]. Only approximately 20% of patients with limited disease can be cured with chemo-radiotherapy, whereas the rest of the patients eventually succumb to the disease.

In SCLC current standard chemotherapy consists of a platinum compound (cisplatin or carboplatin) and etoposide. Doxorubicin is an effective anthracycline chemotherapeutic agent in SCLC, and is widely used in the treatment of numerous other human malignancies, such as breast cancer, bladder cancer, bone and soft tissue sarcoma, multiple myeloma, and lymphoma [4]. In the past, doxorubicin has been used in regimens including cyclophosphamide and vincristine (CAV), or cyclophosphamide and etoposide (CDE) [5], which have similar efficacy to platinum regimens in patients with extensive disease [1]. Recently amrubicin, a second generation anthracycline derivative, has also been shown to have significant activity in SCLC [2]. Other than the intercalation with DNA and inhibition of topoisomerase II causing DNA strand breaks, doxorubicin can also induce interleukin-8 and tumor necrosis factor–alpha (TNF-α) in SCLC [6]. The mechanisms of resistance to doxorubicin are multiple and range from overexpression of P-glycoprotein, to activation of NFkB [7]. Novel agents with more selective mechanisms of action are needed in SCLC. So far no significant activity has been recorded in SCLC with the use of tyrosine kinase inhibitors or other targeted agents, which have significant efficacy in subtypes of non-SCLC and other tumors [8].

Heat Shock Protein 90 (HSP 90) represents an appealing molecular target for the development of novel anticancer therapies. HSP90 is a chaperone protein which has multiple functions, and is involved in response to stress, posttranslational folding, stabilization of mutant oncogenic proteins [9] and plays critical roles in cell growth, differentiation and survival [10]. Tumor cells seem more dependent on HSP90 for proliferation and survival than normal cells, as oncogenic proteins in tumor cells are often misfolded and require high HSP90 activity for correct folding [11]. Thus tumors tend to be more sensitive to HSP90 inhibition as the latter could cause incorrect folding of oncogenic proteins, followed by

proteasome-dependent degradation that leads to cell growth inhibition and death. Over the past decade, several small-molecule inhibitors of the chaperone HSP90 have been developed as potential anticancer agents. Given that numerous oncoproteins have been identified as HSP90 clients (www.picard.ch/downloads/Hsp90interactors.pdf), HSP90 inhibitors have the potential to concomitantly block multiple oncogenic pathways by downregulation of HSP90 client proteins, such as AKT, mTOR, MAPK, epidermal growth factor receptor (EGFR), ErbB2, insulin-like growth factor (IGF)-I, cyclin-dependent kinase 4 (CDK-4) [12], and receptor-interacting serine/threonine-protein kinase 1 (RIP1), etc [13]. The multi-target properties of HSP90 inhibitors have also been shown to be advantageous in terms of overcoming oncogenic signaling redundancies and drug resistance in several cancers types [12]. In this regard, HSP90 inhibition may be of particular benefit to SCLC patients as recent NextGen sequencing studies revealed that SCLC often carries multiple genetic mutations or dysfunctions [14, 15].

Ganetespib (Synta Pharmaceuticals) is a novel small-molecule HSP90 inhibitor with a unique triazolone containing chemical structure, which is different from the benzoquinone structure of the first- and second-generation HSP90 inhibitors, such as geldanamycin and its derivative 17-allylamino-17-demethoxygeldanamycin (17-AAG) [16, 17]. In comparison with 17-AAG, ganetespib is more potent in inducing rapid degradation of HSP90 client proteins and sustaining longer inhibitory activity with short time exposure. While the first generation of HSP90 inhibitors was hampered by poor solubility, significant toxicity and modest efficacy as single agent [18], ganetespib did not display evidence of cardiac, ocular or liver toxicity, observed with other HSP90 inhibitors [16, 17, 19]. Ganetespib demonstrates significant tumor growth inhibition or regression in mouse xenograft models as single agent or in combination therapy [16, 19, 20]. It has shown additive or synergistic activities with agents commonly employed to treat advanced malignances, such as taxanes [20] and etoposide [21]. Preclinical data suggest that HSP90 is the major inhibitor of apoptosis in SCLC, which makes the SCLC cells particularly sensitive to HSP90 inhibition [22]. As a single agent, ganetespib is currently in phase II clinical trial for relapsed or refractory SCLC (NCT01173523) but preliminary results do not appear to show significant antitumor activity (Dr. Leena Gandhi, personal communication).

Here we investigated Ganetespib alone and in combination with doxorubicin in vitro and in vivo in SCLC models. We demonstrate that there is a synergistic interaction in which ganetespib potentiates doxorubicin-induced cell death in part by eliciting persistent G2/M arrest and blocking doxorubicin-induced RIP1 activation.

Results

Ganetespib is more potent than 17-AAG in SCLC cell lines

We examined the single-agent potency of ganetespib in several SCLC cell lines using MTS assay. As shown in Table 1, ganetespib was more potent than the galdanamycin derivative 17-AAG in most of the tested SCLC lines (approximately 200-fold difference in IC50, One-way ANOVA, $p<0.0001$). This is in line with the previous findings of others using a variety of human cell lines[16]. The superior potency of ganetespib over 17-AAG has been attributed to its higher binding affinity to HSP90 and more potent inhibition of HSP90/p23[19].

Moreover, co-crystal structure and computational analysis showed that ganetespib binds to both the closed and open conformations of the ATP pocket lid at the HSP90 N-terminus. In contrast, restricted by their larger sizes, the ansamycin analogues such as 17-AAG can only bind the ATP-binding pocket in the open conformation[16]. The lack of constrain for HSP90 ATP pocket binding may be another reason that ganetespib is more potent than 17-AAG in vitro. Ganetespib significantly inhibited SCLC cell proliferation and induced cell death in vitro as revealed by Trypan Blue Exclusion staining (Fig 1A). As observed in previous preclinical studies in vitro[16], the cytotoxic effect could be observed as early as 24hrs in H69 and H146 cells and 48hrs in GLC4 and H82 cells, respectively.

Ganetespib induces persistent G2/M phase arrest in SCLC cells

Cell cycle analysis (Fig 1B and 1C) showed that ganetespib induced significant dose-dependent cell cycle arrest at G2/M phase in H82 and GLC4 cells. The G2/M arrest was accompanied by concomitant reduction of G1 and S phase cells. Genetespib also induced G2/M phase arrest in other SCLC cell lines N592 (Fig. S1A), H128 and H146 tested (data not shown). Moreover, the G2/M arrest remained persistent 72 hours after ganetespib washout following 30nM ganetespib treatment for 72hrs, in all 3 tested SCLC cell lines (GLC4, H82, H146) (Fig. 1D). Ganetespib stays inside tumor cells even after washout (Dr. Weiwen Ying, Synta Pharmaceuticals, personal communication). The observed persistent G2/M phase arrest may be, in part, due to the persistent presence of ganetespib inside the cells. It is foreseeable that the persistent G2/M arrest may contribute to the observed cell proliferation inhibition and death induced by ganetespib. These findings are consistent with similar reports in non-SCLC cells[16, 20] and confirm that ganetespib exerts strong effects in modulating cell cycle regulatory proteins that are important for its anticancer activity[19, 23].

Ganetespib is synergistic with doxorubicin in vitro

We examined the concomitant combination of ganetespib with two topoisomerase II inhibitors, etoposide and doxorubicin, which have clinical activity in SCLC. MTS assay showed that the IC50 of ganetespib, doxorubicin and etoposide in H82 cells were 30nM, 43nM and 220nM respectively (Table S1). The cell viability was analyzed by TO-PRO-3 stain in cells treated with doxorubicin, ganetespib, etoposide and the combination (ganetespib + doxorubicin or ganetespib + etoposide) (Fig. 2A). In comparison with single treatments (ganetespib, doxorubicin or etoposide), combination treatments (ganetespib + doxorubicin or ganetespib + etoposide) significantly reduced cell viability (p values < 0.05, one-way ANOVA) at all studied time points (24, 48, and 72hrs).

The combinational activity was also assessed by the Chou-Talalay method, using seven different concentrations of ganetespib + doxorubicin or ganetespib + etoposide combinations, in 3 SCLC cell lines, GLC4, H82 and H69 (Figs. 2B and S2). Combination indices (CI) were calculated for each dose combinations. A $CI < 1$ indicated synergy, $CI = 1$ indicated additivity and a $CI > 1$ indicated antagonism. A $CI < 1$ (such as 0.234 for GLC4; 0.67 for H82) was found at low doses of ganetespib and doxorubicin, which inhibited cell growth by more than 70% (Fig. 2B left panel). Similarly, a $CI < 1$ of ganetespib and etoposide (such as 0.654 for GLC4; 0.762 for H82) also led to cell growth inhibition by

more than 70% (Fig. 2B right panel). However, the synergistic activity was less pronounced in H69 cells (Fig S2).

Cytostatic effects of ganetespib + doxorubicin combination treatment

To explore the cytostatic effects of ganetespib + doxorubicin, we examined the cell cycle distribution in cells treated with the indicated concentrations of doxorubicin, ganetespib, and the combination of the two drugs. In combination studies, the cells were either treated concomitantly (drugs added at the same time) or sequentially (ganetespib was supplemented 24hrs after doxorubicin treatment). Similar to H82 and GLC4 cells (Fig. 1B and 1C), all tested SCLC cell lines displayed G2/M phase accumulation 24hrs after ganetespib treatment (Fig 2C, Fig S1A, S1B). N592 and H69 cells showed S and G2/M phase accumulation 24hrs after doxorubicin treatment followed by concomitant S-phase reduction and significant G2/M phase accumulation at 48- and 72-hr time points (Fig. S1A and S1B), indicating that the S accumulation is not permanent, and the cells in S-phase may have died or progressed to G2/M upon the prolonged treatment. In contrast, the observed S and G2/M accumulation was more stable 48 and 72hrs after doxorubicin treatment in H82 cells. In H82 cells, S phase accumulation could be observed 24hrs after concomitant doxorubicin + ganetespib combination treatment followed by S-phase reduction and significant G2/M accumulation, indicating that similar to the effect of doxorubicin treatment in N592 and H69 cells, H82 cells might also have died at S-phase or progressed from S-phase to G2/M in the combination treatment. Similar pattern of S and G2/M oscillation was also observed with sequential combination treatment in N592 and H69 cells, although the S-phase oscillation was not as prominent as with concomitant treatment (Fig. S1A, S1B). Nevertheless, sequential combination treatment blocked cells at G2/M phase as effectively as concomitant combination treatment in H82, N592 and H69 cells (Fig. 2C and Fig. S1A, S1B).

Cytotoxic effects of ganetespib and doxorubicin combination treatment

To examine the cytotoxic effects of the ganetespib + doxorubicin combination, TUNEL staining was performed. More prominent rates of TUNEL-positive cells were found in H82 cells treated with ganetespib (2.45 ± 0.34%) or doxorubicin (3.64 ± 0.48%) than with vehicle (1.35 ± 0.18%). The combination treatment showed the highest rate of TUNEL-positive cells (7.29 ± 0.84%) among all the treatment groups ($P < 0.0001$) (Fig 2D and 2E), indicating that all three regimens elicited cell death, with the combination treatment being the most cytotoxic. Similar results were obtained in GLC4 cells (data not shown). Western blot analysis revealed that Caspase 3 cleavage was more pronounced in H82 and GLC4 cells treated with doxorubicin, ganetespib and the combination than with vehicle alone (Fig. 3A). However, the combination treatment did not significantly augment Caspase 3 cleavage in comparison to doxorubicin or ganetespib single agent treatment, suggesting that part of the observed TUNEL-positive cells (Fig. 2E) in the combination treatment might result from Caspase 3-independent cell death.

To further investigate the molecular mechanism(s) of increased TUNEL-positive cells in the combination treatment, we performed protein expression and phosphorylation profiling by reverse phase protein array (RPPA) analysis with a panel of antibodies against 113 cancer-associated proteins[24, 25]. Unsupervised hierarchical clustering analysis revealed that several

canonical pathways regulating cell cycle, apoptosis/necroptosis, protein synthesis, and RAS/MAPK/AKT were altered in all the treatment groups (Fig. S3A and Table 2). In line with the observed G2/M accumulation, Cyclin B1 (CCNB1)[26], PDK1 (PDPK1) Ser217 phosphorylation and FADD Ser194 phosphorylation[27] were consistently increased, whereas β-Catenin (CTNB1) Thr41Ser45 and Pyk2 (PTK2B) Tyr402 phosphorylations were decreased in doxorubicin, ganetespib and combination treatment groups (Table 2). It is well-established that the DNA damage repair protein poly-(ADP ribose) polymerase (PARP) is cleaved and inactivated by Caspase 3/7 in Caspase 3/7-dependent apoptosis[28]. In our analysis, cleaved PARP was significantly augmented 48hrs after the combination treatment (Table 2), and western blot analysis showed that cleaved Caspase 3 was constantly elevated in all three treatment groups (Fig. 3A). To further discern proteins that may mediate the effects of ganetespib + doxorubicin combination treatment, we applied our RPPA data to Ingenuity Interactive Pathway (IPA) analysis using available published protein interaction data. RIP1 (RIPK1) was found to be in the apoptosis/necroptosis networks, where it shows direct interaction with its known interacting-protein FADD[13] and chaperone HSP90[29] (Fig. S3B), in which the former was altered in our experimental settings (Table 2) and the latter was inhibited by ganetespib. It has been shown that RIP1 acts as a survival or necroptotic signal when apoptosis pathway is blocked in TNFR1-activated cells[30, 31]. Interestingly, we showed that doxorubicin upregulated whereas ganetespib downregulated RIP1 in both H82 and GLC4 cells by western blot analysis (Fig. 3A). As a control, 17-AAG, a geldanamycin derivative which is different in structure from ganetespib, could also suppress RIP1 expression in GLC4 cells, albeit to a lesser extent than ganetespib (Fig. S4), indicating that the RIP1 inhibition was potentially the on-target effect of HSP90 inhibitions. This is in agreement with the stronger growth inhibitory potency of ganetespib as compared to 17-AAG as illustrated earlier. To evaluate the significance of RIP1 upregulation in doxorubicin-treated cells, we depleted RIP1 using siRNA-mediated knockdown approach in doxorubicin-treated H82 and GLC4 cells (Fig. 3B). Interestingly, knockdown of RIP1 by RIP1 #1 or #4 siRNAs sensitized doxorubicin-mediated cell death (Fig. 3 C–D and Fig. S5) to a similar extent as ganetespib + doxorubicin combination treatment (Fig. 2A), suggesting that RIP1 may confer a survival signal and disruption of RIP1 may be essential in mediating the synergistic effect.

Synergistic effect of ganetespib and doxorubicin combination in SCLC xenograft model

H82 xenografts in immunodeficient nude mice were treated with ganetespib and doxorubicin, both as single agent and combination. As shown in Fig. 4A, weekly intravenous administration of the non-toxic dose[16, 19] of ganetespib of 150mg/kg induced tumor regression with a T/C value of 36.1%. Doxorubicin single-agent treatment with 4mg/kg intraperitoneally every other day had a T/C value of 38.9%. Consistent with the in vitro findings, combination treatment with the same comparable doses and schedules as its respective single agents resulted in a significantly improved tumor volume reduction with a T/C value of 14.1%. ($P < 0.0001$; One-way ANOVA). This was accompanied by a prominent reduction of RIP1 expression in the combination group which was apparently mediated by ganetespib treatment (Fig. 4B) as documented in our in vitro studies (Fig. 3A). Though not as prominent as in H82 xenografts, the combination treatment also significantly reduced tumor volumes with a %T/C value of 37.2 ($p<0.008$) in GLC4 xenograft experiments (Fig.

S6), validating our finding in another SCLC xenograft model system. Single-agent ganetespib was well tolerated with increase in body weight of 6.24%. The body weight loss of mice treated with single agent doxorubicin and combination therapy were −0.35% and −5.04%, respectively (Fig. S7).

Ganetespib and doxorubicin combination treatment causes more cell death than single agents in xenograft tumors

The xenografts were stained with hematoxylin and eosin. In xenografts treated with doxorubicin, there were extensive areas of necrosis, and similar rates of necrotic cells were found in tumors of genetespib treatment group (Fig. 4C). In addition, many cells of ganetespib-treated xenografts were larger in size with cytoplasmic vacuoles, indicative of G2/M arrest or dying cells. The presence of G2/M-arrested cells in ganetespib, doxorubicin and combination treatment groups were revealed by the accumulation of G2/M phase marker Survivin[32]. As documented in in-vitro experiments (Fig. 3A), the response to HSP90 inhibition was monitored by HSP70 accumulation[18] (Fig. 4B). Importantly, multi-section evaluation of the H&E stained slides showed that the doxorubicin + ganetespib combination-treated cells looked smaller than the genetespib- or doxorubicin-treated cells, which was in line with the finding that xenograft tumors in the combination treatment group exhibited higher rate of necrotic cells than either single agent treatment groups (Fig. 4C).

Discussion

In this study, we demonstrated that ganetespib is a potent HSP90 inhibitor in SCLC cells, and that ganetespib and doxorubicin are synergistic in vitro and in SCLC xenograft models.

HSP90 inhibition initiates G1/G0 arrest in Rb-positive cells. In contrast to the DNA-damaging drug doxorubicin, inhibition of HSP90 in many Rb-negative cell lines has no effects on cell cycle progression, or induces slight accumulation at the G2/M checkpoint[33]. Most of the SCLC cell lines employed in this study are Rb-negative (Table S2). The fact that ganetespib elicited G2/M arrest in the tested SCLC cell lines raises the possibility that ganetespib, like doxorubicin, may cause DNA damage which in turns triggers G2/M checkpoint arrest. However, we did not see significant induction of the DNA damage marker γH2AX in ganetespib- or 17-AAG-treated GLC4 and H82 cells (Figs. S4 and S8), suggesting that ganetespib may not induce G2/M arrest via damaging DNA. Many G2/M regulators, such as Cyclin B, Cdc2 and Cdc25 are known HSP90 client proteins (www.picard.ch/downloads/Hsp90interactors.pdf). It remains to be investigated whether degradation of those regulatory proteins may also play a role in ganetespib-induced G2/M arrest.

Although previous studies showed that geldanamycin analogs DMAG and 17AAG synergized with doxorubicin by abrogating doxorubicin-induced G2/M arrest via downregulation of Chk1 followed by apoptosis in p53 mutant lymphoma and leukemia cell lines[34, 35], contradictory results were reported in other p53-null HL60 and U937 cells[36, 37]. In this study, ganetespib synergized with doxorubicin in the absence of G2/M checkpoint abrogation in the p53 mutant/RB negative H82 and H69 cells, suggesting that synergistic mechanism(s) may vary in different cell types.

In general, HSP90 inhibitor-induced cell cycle arrest has been thought to be reversible, although this issue has not been thoroughly addressed. In a subset of cancers, such as SCLC and multiple myeloma cells, it has been shown that HSP90 inhibitors induce apoptosis[22, 38]. We observed two distinct responses to ganetespib: cell cycle arrest and cell death. Ganetespib-induced G2/M arrest was persistent 72 hrs after drug washout or 6 days from the start of drug treatment (Fig. 1D). It is plausible that the high potency of ganetespib in most of the cancer cell lines tested[17, 18, 39, 40] may in part be attributed to its persistent cell cycle arrest.

RIP1 is an HSP90 client protein[13] and known to interact with FADD [29]. FADD Ser194 phosphorylation was altered in all the treatment groups in our study (Table 2). Ingenuity pathway analysis of our RPPA data revealed that RIP1 may be involved in the apoptotic/necroptotic response of doxorubicin and ganetaspib treated SCLC cells. In line with this, we showed that RIP1 expression was upregulated in doxorubicin-treated SCLC cells. Depletion of RIP1 by siRNA enhanced cell death induced by doxorubicin, suggesting that the role of RIP1 in this experimental setting may be to mediate a survival signal. As disruption of HSP90 function by ganetespib caused significant reduction of RIP1 expression (Fig. 3A), one of the potential mechanisms by which ganetespib synergizes with doxorubicin in inhibiting SCLC cell growth may be through downregulation of RIP1. High expression of RIP1 has been reported to contribute to resistance to TNFα-induced apoptosis through activation of NFkB pathway[13], probably via regulation of IκB degradation[41]. Doxorubicin has been reported to induce NFkB activation, which may render cells either resistant[7] or sensitive[42] to the drug. It is conceivable that ganetespib could counteract the effect of doxorubicin on NFkB activity, as western blot analysis revealed that doxorubicin modestly decreased and ganetespib increased the abundance of IκB-α, an inhibitor of NFkB pathway[41] in GLC4 cells (Fig. S9A). However, siRNA-mediated RIP1 depletion did not significantly alter the abundance of IκB-α (Fig. S9B), suggesting that the negative effect of ganetespib on NFkB activation, if any, may not require RIP1. How the downregulation of RIP1 by ganetespib may play a role in doxorubicin sensitization will require additional investigation. Taken altogether, our data suggest that ganetespib may sensitize doxorubicin-induced cell death in part through inhibition of RIP1 activity and induction of persistent G2/M phase arrest.

Combination chemotherapy remains the mainstay treatment for most tumors. Standard first line chemotherapy regimens for SCLC include platinum containing doublet regimens (etoposide and cisplatin or carboplatin, and irinotecan and cisplatin mainly in Japan)[43, 44], and also doxorubicin containing regimens (cyclophosphamide, doxorubicin, and vincristine, CAV[45, 46], and cyclophosphamide, doxorubicin, etoposide, CDE[43, 44]. Platinum doublets have been preferred more recently because of easier coadministration with radiation therapy in patients with limited disease. SCLC patients are highly sensitive to initial chemotherapy, however, the overall prognosis has improved little over the past two decades, mainly because the response to treatment is often short and the prognosis of relapsed patients who receive second-line therapy, such as topotecan or CAV, is poor[1, 47]. The novel anthracycline amrubicin has been shown to have definite antitumor activity in platinum-refractory SCLC[48], but randomized studies in second line and in first line have failed to show significant advantages against standard chemotherapy[49].

The mechanisms of resistance to chemotherapies are still largely unknown[50], and there is an urgent need to develop more effective first- and second-line therapeutic regimens that would circumvent these resistant mechanisms. In this study, we showed that ganetespib and doxorubicin combination exhibited significant synergy in inhibiting the growth of SCLC cells in vitro and in mouse xenografts. The efficacy of the combination treatment and the potential involvement of RIP1 to mediate the synergy discovered in this study suggest that ganetespib may enhance the effects of doxorubicin and potentially attenuate the occurrence of resistance. Clinical studies of a combination of ganetespib and doxorubicin are warranted in SCLC patients with extensive disease.

Materials and Methods

Cell lines and drugs

All SCLC cell lines (GLC4, NCI-H82, NCI-H69, NCI-H128, NCI-H146, NCI-H187, NCI-H526, NCI-N592, NCI-H620, NCI-H792, NCI-H1173, and AC-3) were cultured in RPMI-1640 media supplemented with 10% fetal bovine serum (FBS) at 37°C in 5%CO_2 incubator. Cell viability was assessed by Trypan Blue staining (Life technologies, Grand Island, NY). Doxorubicin (LC Laboratories, Woburn, MA), etoposide (Sigma-Aldrich, St. Louis, MO) and ganetespib (STA-9090) (Synta Pharmaceuticals, Lexington, MA) were dissolved in DMSO according to the manufacturer's instructions.

Cell cycle analysis

Cells were seeded in 25cm^2-flasks at a density of 2×10^5 cells/ml. Before collection, cells were washed with cold phosphate buffered saline (PBS) and fixed with cold 70% ethanol in PBS followed by centrifugation. Cell pellets were resuspended in 500 μl propidium iodine in PBS (10 μg/ml) containing 300 μg/ml RNase (Qiagen, Valencia, CA). Cells were then incubated for 30min with gentle shaking and filtered with 40 μm nylon mesh (BD Falcon, CA). Cells were acquired by FACScalibur using Cellquest Pro software (Becton Dickinson and Company, Franklin Lakes, NJ) and cell cycle distributions were analyzed using ModFit LT™ software (Verity Software House, Topsham, ME).

siRNA transfection

Four different RIP1 small interfering RNAs (siRNA): # 1 (SI00288092:TACCACTAGTCTGACGGATAA), #2 (SI02621983:CCGACATTTCCTGGCATTGAA), #3 (SI04437860:TCCGTTAACGTTAATACCCAA), #4 (SI00056014:CAGCTGCTAAGTACCAAGCTA); negative control siRNA (Catalog no. 1027281) and cell death control siRNA (Catalog no. 10272299) were purchased from Qiagen (Valencia, CA). Transfection of siRNA was carried out using 0.2% Lipofectamine (Life technologies, Grand Island, NY). H82 and GLC4 cells were seeded at a density of 3×10^5 cells/ml in a 6-well tissue culture dish and transfected with siRNA-Lipofectamine mixture (5nM, 10nM or 15nM siRNA).

TO-PRO-3 viability assay

10^6 cells were harvested by centrifugation and washed in PBS twice. TO-PRO 3™ iodide (Life technologies, Grand Island, NY) was added at a final concentration of 500nM to the cells in PBS immediately before analysis. Cells were acquired using a FACSCalibur flow cytometer (Beckton Dickinson) and analyzed by FlowJo (Tree Star, Ashland. OR).

MTS assay

Briefly, 20,000 cells in 200μl media were dispensed into each well of 96-well flat-bottom plates. Plates were subsequently incubated for 72hrs with different concentrations of drugs. 10μl of MTS (3-(4,5-dimethylthiazol-2-yl)-5-(3-carboxymethoxyphenyl)-2-(4-sulfophenyl)-2H-tetrazolium) reagent was added to each well. Two or three hours later, absorbance at 490nm was measured by a multi-well plate reader (Molecular Devices, Sunnyvale, CA). Experiments were repeated at least three times. The cell viability was obtained by normalizing the absorbance of the treated samples with that of the controls and expressed as percentage, assigning the viability of non-treated cells as 100%. Survival curves were constructed using Prism V5.0 (GraphPad Software, La Jolla, CA), and IC50s were calculated.

Cytotoxic combination effects of doxorubicin, etoposide and ganetespib were assessed with 7 different concentrations of drugs (3.75, 2.25, 1.5, 1, 0.67, 0.44, and 0.27 × IC50). Combination indexes (CI) were calculated using CalcuSyn (Biosoft, UK). The Chou-Talalay method was used, that defines additive effect (CI = 1), synergism (CI < 1), and antagonism (CI > 1) of drug combinations [51].

Western blot and antibodies

Following treatment, tumor cells were harvested, centrifuged and washed with cold PBS. Lysates were prepared with RIPA buffer on ice, equal amounts of proteins were dissolved in SDS-PAGE and Western blot was performed as described previously [52]. The intensities of band signals were assessed using GeneTools software (SynGene, Frederick, MD) and normalized by the intensity of α-tubulin. All antibodies were purchased from Cell Signaling Technology (Danvers, MA).

In vivo xenograft tumor models and drug administrations

Two-week-old athymic immunodeficient nude mice were maintained in the pathogen-free facilities of the National Institutes of Health (NIH), and cared in accordance with the NIH Guide for the Care and Use of Laboratory Animals. Mice were subcutaneously implanted with 8×10^6 NCI-H82 or GLC4 cells and left to grow for 2 weeks to a volume of about 80–100mm^3. Eligible mice were randomized into treatment groups of 8. Doxorubicin was administered by intraperitoneal injection of 4mg/kg, 3-times a week for 3 weeks. Ganetespib (STA-12-1474 for *in vivo* study from Synta Pharmaceuticals) [16, 20], formulated in PBS and PH-adjusted to neutral just before use in order to prevent precipitation, was injected intravenously via tail vein. Mice were treated with ganetespib at 150 mg/kg weekly for 3 weeks.

Animals were closely monitored and body weight and tumor volume were measured 3 times a week. Tumor volumes were calculated using $V=1/2(L \times W^2)$ formula. The T/C value was determined from changes in average tumor volumes of drug-treated groups relative to vehicle-treated groups.

TUNEL stain

Approximately 10^6 cells treated with 40nM doxorubicin, 30nM ganetespib, 40nM doxorubicin + 30nM ganetespib combination or vehicle, were harvested, centrifuged, washed in PBS, resuspended with 30 μl PBS and added to poly-L-lysine-coated slides, and left to air-dry in a tissue culture hood for approximately 1–2hrs before fixation. The terminal deoxynucleotidyl transferase dUTP nick end labeling (TUNEL) was performed using the DeadEnd™ Colorimetric TUNEL System Kit (Promega, Madison, WI), following the manufacturer's protocol.

Reverse Phase Protein Array (RPPA) analysis

H82 cells were treated with 40nM doxorubicin, 30nM ganetespib, 250nM etoposide, the combination of 40nM doxorubicin + 30nM ganetespib, or 250nM etoposide + 30nM ganetespib for 24 and 48hrs respectively. Cell lysates were prepared as previously described [53]. Samples derived from drug treatment and control groups were printed in triplicates onto the same arrays of nitrocellulosecoated slides, and probed with 113 antibodies targeting cancer-associated total and phosphorylated proteins respectively as described previously [24, 25]. Final signal intensities were obtained after background, secondary antibody subtraction and normalization to the total amount of protein present in each individual samples [53].

Statistical analysis

Statistical analysis was performed using SPSS version 17.0 (SPSS, Chicago, IL) or GraphPad Prism V5.0 (GraphPad Software, La Jolla, CA). Comparisons of categorical variables between the different groups were made using the chi-square test or Fisher's exact test, when the number of cases was fewer than five. The paired Student's *t* test for continuous variables was performed for means between paired groups. Comparison of drug efficacy and potency in different treatment groups was carried out by one-way analysis of variances (ANOVA). All p values were two-sided and p values of < 0.05 were regarded as significant.

For RPPA data analysis, the Ward method for two-way unsupervised hierarchical clustering was performed using JMP v5.1 (SAS Institute, Cary, NC). One-way ANOVA with Dunnett's Multiple Comparison Test (Prism v5.0b, GraphPad Software, Inc., La Jolla, CA) was applied to compare values of treatment groups with those of control group. P values < 0.05 were considered statistically significant.

Supplementary Material

Refer to Web version on PubMed Central for supplementary material.

Acknowledgments

Grant Support: National Cancer Institute Intramural Program funded this research

We thank Dr. Leonard M. Neckers for stimulating discussion during the course of the study and Dr. Weiwen Ying (Synta Pharmaceuticals) for his valuable comments on the manuscript and providing ganetespib for the study.

References

1. Jackman DM, Johnson BE. Small-cell lung cancer. Lancet. 2005; 366:1385–1396. [PubMed: 16226617]
2. Schmittel A. Second-line therapy for small-cell lung cancer. Expert Rev Anticancer Ther. 2011; 11:631–637. [PubMed: 21504329]
3. Lally BE, Urbanic JJ, Blackstock AW, Miller AA, Perry MC. Small cell lung cancer: have we made any progress over the last 25 years? Oncologist. 2007; 12:1096–1104. [PubMed: 17914079]
4. Singhal SS, et al. Determinants of differential doxorubicin sensitivity between SCLC and NSCLC. FEBS Lett. 2006; 580:2258–2264. [PubMed: 16579994]
5. von Pawel J, et al. Topotecan versus cyclophosphamide, doxorubicin, and vincristine for the treatment of recurrent small-cell lung cancer. J Clin Oncol. 1999; 17:658–667. [PubMed: 10080612]
6. Shibakura M, et al. Induction of IL-8 and monoclyte chemoattractant protein-1 by doxorubicin in human small cell lung carcinoma cells. Int J Cancer. 2003; 103:380–386. [PubMed: 12471621]
7. Gangadharan C, Thoh M, Manna SK. Inhibition of constitutive activity of nuclear transcription factor kappaB sensitizes doxorubicin-resistant cells to apoptosis. J Cell Biochem. 2009; 107:203–213. [PubMed: 19242952]
8. Califano R, Abidin AZ, Peck R, Faivre-Finn C, Lorigan P. Management of small cell lung cancer: recent developments for optimal care. Drugs. 2012; 72:471–490. [PubMed: 22356287]
9. Calderwood SK, Khaleque MA, Sawyer DB, Ciocca DR. Heat shock proteins in cancer: chaperones of tumorigenesis. Trends Biochem Sci. 2006; 31:164–172. [PubMed: 16483782]
10. Whitesell L, Lindquist SL. HSP90 and the chaperoning of cancer. Nat Rev Cancer. 2005; 5:761–772. [PubMed: 16175177]
11. Kamal A, et al. A high-affinity conformation of Hsp90 confers tumour selectivity on Hsp90 inhibitors. Nature. 2003; 425:407–410. [PubMed: 14508491]
12. Xu W, Neckers L. Targeting the molecular chaperone heat shock protein 90 provides a multifaceted effect on diverse cell signaling pathways of cancer cells. Clin Cancer Res. 2007; 13:1625–1629. [PubMed: 17363512]
13. Lewis J, et al. Disruption of hsp90 function results in degradation of the death domain kinase, receptor-interacting protein (RIP), and blockage of tumor necrosis factor-induced nuclear factor-kappaB activation. J Biol Chem. 2000; 275:10519–10526. [PubMed: 10744744]
14. Sos ML, et al. A framework for identification of actionable cancer genome dependencies in small cell lung cancer. Proc Natl Acad Sci U S A. 2012; 109:17034–17039. [PubMed: 23035247]
15. Rudin CM, et al. Comprehensive genomic analysis identifies SOX2 as a frequently amplified gene in small-cell lung cancer. Nat Genet. 2012; 44:1111–1116. [PubMed: 22941189]
16. Ying W, et al. Ganetespib, a unique triazolone-containing Hsp90 inhibitor, exhibits potent antitumor activity and a superior safety profile for cancer therapy. Mol Cancer Ther. 2012; 11:475–484. [PubMed: 22144665]
17. Wang Y, Trepel JB, Neckers LM, Giaccone G. STA-9090, a small-molecule Hsp90 inhibitor for the potential treatment of cancer. Curr Opin Investig Drugs. 2010; 11:1466–1476.
18. Kim YS, et al. Update on Hsp90 inhibitors in clinical trial. Curr Top Med Chem. 2009; 9:1479–1492. [PubMed: 19860730]
19. Shimamura T, et al. Ganetespib (STA-9090), a Non-Geldanamycin HSP90 Inhibitor, has Potent Antitumor Activity in In Vitro and In Vivo Models of Non-Small Cell Lung Cancer. Clin Cancer Res. 2012

20. Proia DA, et al. Synergistic activity of the Hsp90 inhibitor ganetespib with taxanes in non-small cell lung cancer models. Invest New Drugs. 2012
21. Bansal H, et al. Heat shock protein 90 regulates the expression of Wilms tumor 1 protein in myeloid leukemias. Blood. 2010; 116:4591–4599. [PubMed: 20651072]
22. Rodina A, et al. Selective compounds define Hsp90 as a major inhibitor of apoptosis in small-cell lung cancer. Nat Chem Biol. 2007; 3:498–507. [PubMed: 17603540]
23. Proia DA, et al. Multifaceted intervention by the Hsp90 inhibitor ganetespib (STA-9090) in cancer cells with activated JAK/STAT signaling. PLoS One. 2011; 6:e18552. [PubMed: 21533169]
24. Nishizuka S, et al. Proteomic profiling of the NCI-60 cancer cell lines using new high-density reverse-phase lysate microarrays. Proc Natl Acad Sci U S A. 2003; 100:14229–14234. [PubMed: 14623978]
25. Sheehan KM, et al. Signal pathway profiling of epithelial and stromal compartments of colonic carcinoma reveals epithelial-mesenchymal transition. Oncogene. 2008; 27:323–331. [PubMed: 17621268]
26. Choi HJ, Fukui M, Zhu BT. Role of cyclin B1/Cdc2 up-regulation in the development of mitotic prometaphase arrest in human breast cancer cells treated with nocodazole. PLoS One. 2011; 6:e24312. [PubMed: 21918689]
27. Scaffidi C, et al. Phosphorylation of FADD/MORT1 at serine 194 and association with a 70-kDa cell cycle-regulated protein kinase. J Immunol. 2000; 164:1236–1242. [PubMed: 10640736]
28. Chaitanya GV, Steven AJ, Babu PP. PARP-1 cleavage fragments: signatures of cell-death proteases in neurodegeneration. Cell Commun Signal. 2010; 8:31. [PubMed: 21176168]
29. Zhang H, et al. Functional complementation between FADD and RIP1 in embryos and lymphocytes. Nature. 2011; 471:373–376. [PubMed: 21368761]
30. Mahoney DJ, et al. Both cIAP1 and cIAP2 regulate TNFalpha-mediated NF-kappaB activation. Proc Natl Acad Sci U S A. 2008; 105:11778–11783. [PubMed: 18697935]
31. Varfolomeev E, et al. c-IAP1 and c-IAP2 are critical mediators of tumor necrosis factor alpha (TNFalpha)-induced NF-kappaB activation. J Biol Chem. 2008; 283:24295–24299. [PubMed: 18621737]
32. Chandele A, Prasad V, Jagtap JC, Shukla R, Shastry PR. Upregulation of survivin in G2/M cells and inhibition of caspase 9 activity enhances resistance in staurosporine-induced apoptosis. Neoplasia. 2004; 6:29–40. [PubMed: 15068669]
33. Srethapakdi M, Liu F, Tavorath R, Rosen N. Inhibition of Hsp90 function by ansamycins causes retinoblastoma gene product-dependent G1 arrest. Cancer Res. 2000; 60:3940–3946. [PubMed: 10919672]
34. Robles AI, et al. Schedule-dependent synergy between the heat shock protein 90 inhibitor 17-(dimethylaminoethylamino)-17-demethoxygeldanamycin and doxorubicin restores apoptosis to p53-mutant lymphoma cell lines. Clin Cancer Res. 2006; 12:6547–6556. [PubMed: 17085670]
35. Sugimoto K, et al. Hsp90-inhibitor geldanamycin abrogates G2 arrest in p53-negative leukemia cell lines through the depletion of Chk1. Oncogene. 2008; 27:3091–3101. [PubMed: 18071310]
36. Blagosklonny MV, et al. The Hsp90 inhibitor geldanamycin selectively sensitizes Bcr-Abl-expressing leukemia cells to cytotoxic chemotherapy. Leukemia. 2001; 15:1537–1543. [PubMed: 11587211]
37. Demidenko ZN, et al. Pharmacological induction of Hsp70 protects apoptosis-prone cells from doxorubicin: comparison with caspase-inhibitor- and cycle-arrest-mediated cytoprotection. Cell Death Differ. 2006; 13:1434–1441. [PubMed: 16311509]
38. Davenport EL, et al. Heat shock protein inhibition is associated with activation of the unfolded protein response pathway in myeloma plasma cells. Blood. 2007; 110:2641–2649. [PubMed: 17525289]
39. Banerji U, Judson I, Workman P. The clinical applications of heat shock protein inhibitors in cancer - present and future. Curr Cancer Drug Targets. 2003; 3:385–390. [PubMed: 14529390]
40. Powers MV, Workman P. Targeting of multiple signalling pathways by heat shock protein 90 molecular chaperone inhibitors. Endocr Relat Cancer. 2006; 13 (Suppl 1):S125–135. [PubMed: 17259553]

41. Declercq W, Vanden Berghe T, Vandenabeele P. RIP kinases at the crossroads of cell death and survival. Cell. 2009; 138:229–232. [PubMed: 19632174]
42. Bian X, et al. NF-kappa B activation mediates doxorubicin-induced cell death in N-type neuroblastoma cells. J Biol Chem. 2001; 276:48921–48929. [PubMed: 11679590]
43. Roth BJ, et al. Randomized study of cyclophosphamide, doxorubicin, and vincristine versus etoposide and cisplatin versus alternation of these two regimens in extensive small-cell lung cancer: a phase III trial of the Southeastern Cancer Study Group. J Clin Oncol. 1992; 10:282–291. [PubMed: 1310103]
44. Fukuoka M, et al. Randomized trial of cyclophosphamide, doxorubicin, and vincristine versus cisplatin and etoposide versus alternation of these regimens in small-cell lung cancer. J Natl Cancer Inst. 1991; 83:855–861. [PubMed: 1648142]
45. Sculier JP, et al. A phase II study evaluating CAVi (cyclophosphamide, adriamycin, vincristine) potentiated or not by amphotericin B entrapped into sonicated liposomes, as salvage therapy for small cell lung cancer. Lung Cancer. 1990; 6:110–118.
46. Shepherd FA, Evans WK, MacCormick R, Feld R, Yau JC. Cyclophosphamide, doxorubicin, and vincristine in etoposide- and cisplatin-resistant small cell lung cancer. Cancer Treat Rep. 1987; 71:941–944. [PubMed: 2820571]
47. Pelayo Alvarez M, Gallego Rubio O, Bonfill Cosp X, Agra Varela Y. Chemotherapy versus best supportive care for extensive small cell lung cancer. Cochrane Database Syst Rev. 2009:CD001990. [PubMed: 19821287]
48. Ettinger DS, et al. Phase II study of amrubicin as second-line therapy in patients with platinum-refractory small-cell lung cancer. J Clin Oncol. 2010; 28:2598–2603. [PubMed: 20385980]
49. Kotani, Yoshikazu, et al. A phase III study comparing amrubicin and cisplatin (AP) with irinotecan and cisplatin (IP) for the treatment of extended-stage small cell lung cancer (ED-SCLC): JCOG0509. J Clin Oncol (Meeting Abstracts). 2012; 30(suppl):7003.
50. Cook RM, Miller YE, Bunn PA Jr. Small cell lung cancer: etiology, biology, clinical features, staging, and treatment. Curr Probl Cancer. 1993; 17:69–141. [PubMed: 8395998]
51. Chou TC. Drug combination studies and their synergy quantification using the Chou-Talalay method. Cancer Res. 2010; 70:440–446. [PubMed: 20068163]
52. Park KS, et al. TNF-alpha mediated NF-kappaB activation is constantly extended by transglutaminase 2. Front Biosci (Elite Ed). 2011; 3:341–354. [PubMed: 21196314]
53. Pierobon M, Vanmeter AJ, Moroni N, Galdi F, Petricoin EF. md Reverse-phase protein microarrays. Methods Mol Biol. 2012; 823:215–235. [PubMed: 22081348]

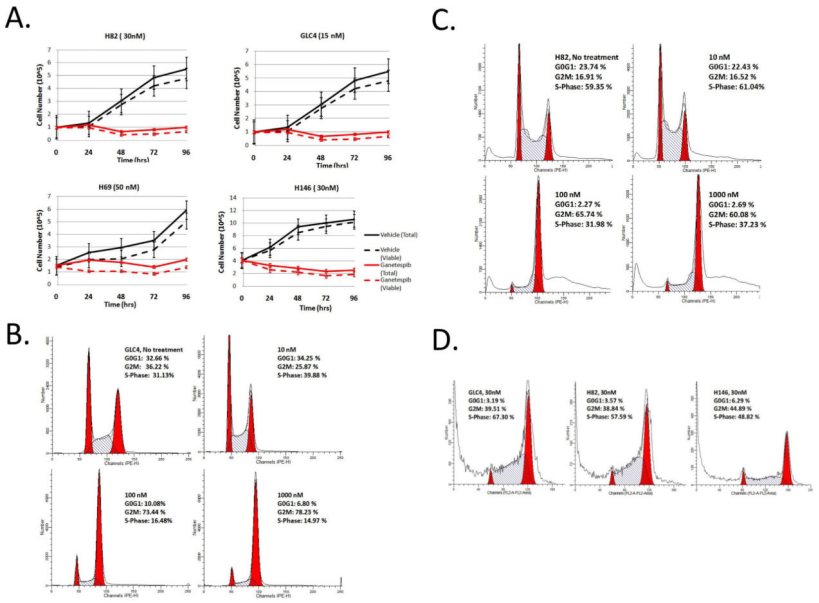

Figure 1.

A. Cell counts of SCLC cells treated with vehicle (black lines) or with ganetespib at IC50 concentration (red lines), at the indicated time points. Solid lines represent total number of cells, whereas dotted lines represent viable cells, as counted by Trypan blue staining. The data were derived from three independent experiments. Bars indicate standard errors. **B. & C.** G2/M phase arrest of GLC4 and H82 cells 24-hrs after ganetespib treatment at the indicated concentrations. **D.** Cells were treated with ganetespib for 72 hrs followed by drug washout for another 72 hrs. Note that ganetespib-induced G2/M arrest is still present 72 hours after ganetespib washout in H82, GLC4 and H146 cells.

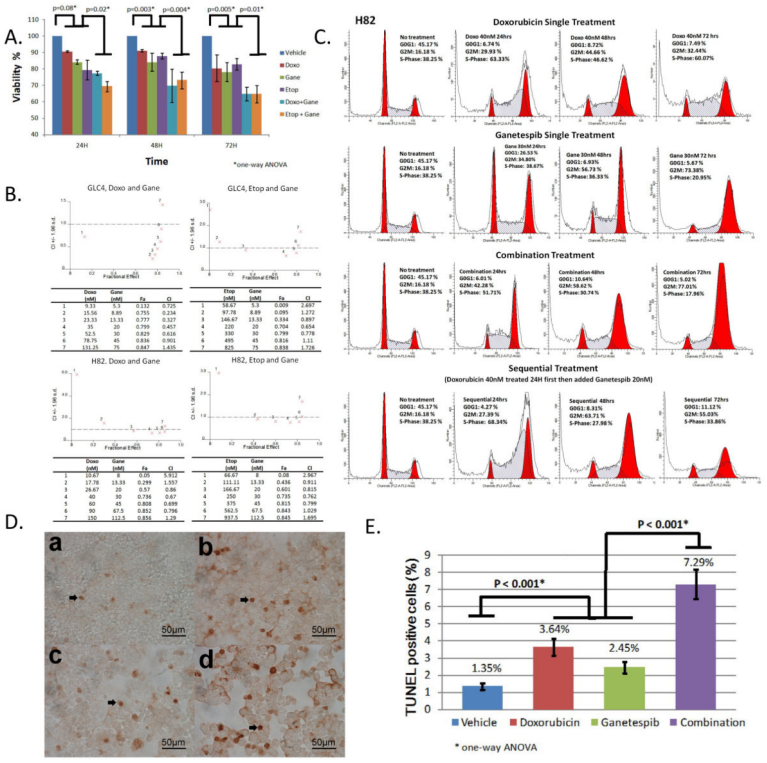

Figure 2.

A. TO-PRO-3 staining in H82 cells treated with 40 nM doxorubicin (Doxo), 30 nM ganetespib (Gane), 250nM etoposide (Etop), 40 nM Doxo + 30 nM Gane and 250 nM Etop + 30 nM Gane. TO-PRO-3 stain was performed at 24, 48, and 72 hours after drug treatment. Data summarize 3 independent experiments. P value was calculated by one-way ANOVA test. **B.** Synergy of doxorubicin + ganetespib or etoposide + ganetespib combinations was observed in GLC4 and H82 cells by MTS assay. Combination index (CI) was calculated using Calcusyn algorithm (see Materials and Methods). CI of < 1.0 represents synergy. Each number (1 to 7) in the graph represents drug concentrations from top to bottom in the table. Number 4 is IC50 of each drug in both cell lines. **C.** Cell cycle analysis of H82 cells treated with doxorubicin (IC50= 40 nM), genetespib (IC50=30 nM) and the combination. **D.** TUNEL staining of H82 cells 24hrs after the following treatment: a. vehicle; b. doxorubicin 40nM; c. ganetespib 30nM; d. 40nM doxorubicin + 30nM ganetespib. Arrowheads indicate TUNEL positive cells. 400X magnification**. E.** Quantification of TUNEL staining in H82 cell lines treated with the indicated drugs for 24 hours. Each column represents means ± SD of at least three independent experiments.

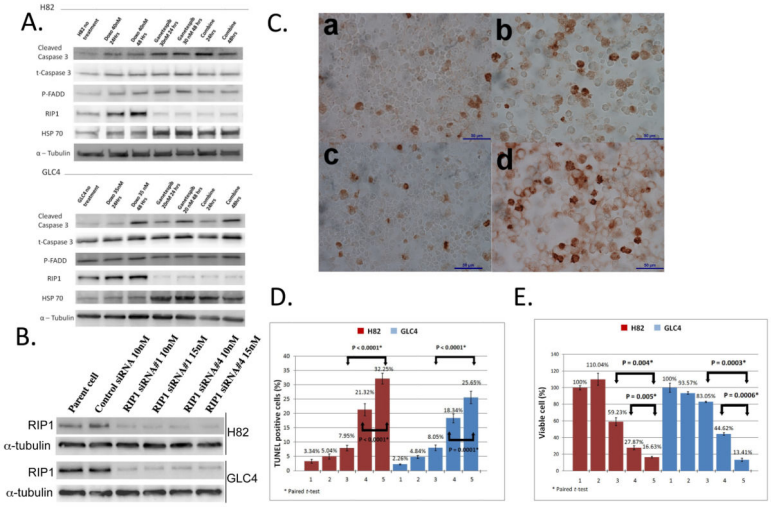

Figure 3.

A. Western blot analysis of H82 and GLC4 cells treated with the indicated drugs after 24h and 48h exposure**. B.** Western blot analysis of H82 and GLC4 cells transfected with 10nM or 15nM of control or RIP1 siRNAs for 72 hrs. **C.** TUNEL staining of H82 cells 72 hrs after the following treatment: a. Negative control siRNA; b. Doxorubicin (40nM); c. RIP1 siRNA (5nM); d. Doxorubicin (40nM) and RIP1 (5nM) siRNA combination. Note that lipofectamine was added in doxorubicin treatment group as a transfection reagent control. 400X magnification. **D.** Quantification of TUNEL staining in H82 and GLC4 cells. Each column represents means ± SD of at least three independent experiments. The columns are: 1. 0.2% Lipofectamine 72 hours; 2. Control siRNA 5nM (H82), 10nM (GLC4) 72 hours; 3. RIP1 siRNA 5nM (H82), 10nM (GLC4) 72 hours; 4. 0.2% Lipofectamine 72 hours plus doxorubicin 40nM 48 hours; 5. RIP1 siRNA 5nM (H82), 10nM (GLC4) 72 hours plus doxorubicin 40nM 48 hours**. E.** Percentage of viable H82 and GLC4 cells. Bars indicate standard errors. Column numbers are the same as in D.

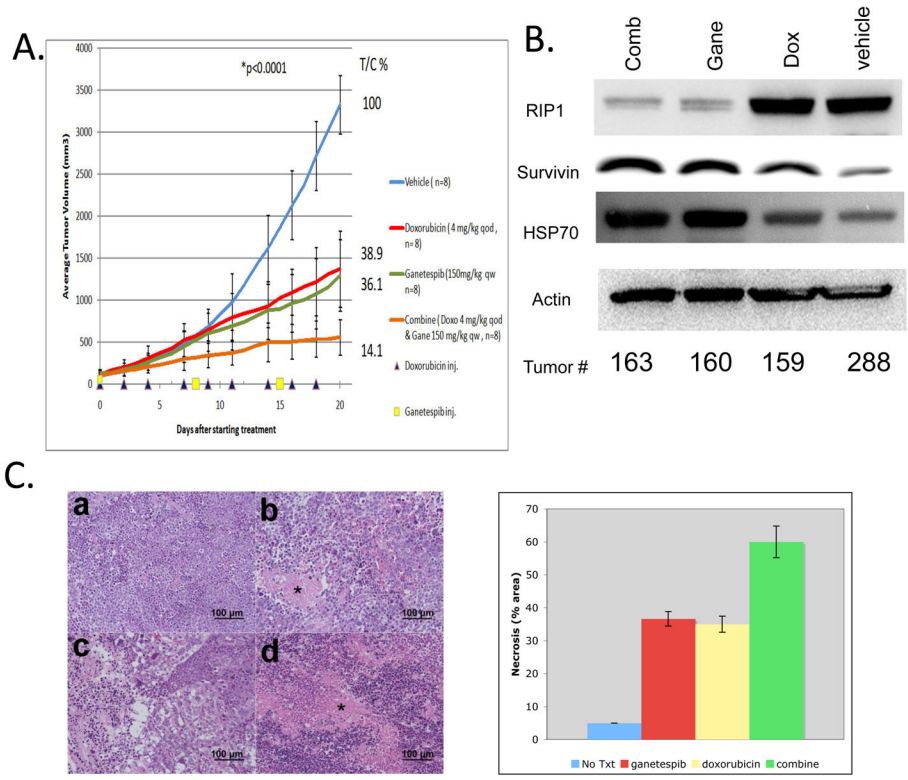

Figure 4.

A. Mouse xenograft study of H82 cells. p-value was calculated by one-way ANOVA at day 20 after drug treatment. p values were significant between any two group comparisons except for the doxorubicin and ganetespib comparison. %T/C value was calculated at the end of the experiment according to the following formula: $(\Delta\text{treated tumor volume}/\Delta\text{control tumor volume}) \times 100$, where Δtumor volume represents the mean tumor volume on the evaluation day minus the mean tumor volume at the start of the experiment. Bars indicate standard errors. Drug doses and schedules are indicated in the graph. **B.** Western blot analysis of H82 xenograft tumors harvested at the end of drug treatment experiments. **C.** H&E stain of H82 xenograft tumors. a. Vehicle; b. Doxorubicin 4mg/kg treated every other day; c. Ganetespib 150mg/kg treated every week; d. Combination treatment. * Necrosis; 200X. Quantitations of necrosis (% area on H&E stained slides) by a pathologist (M.R.) are shown on the right.

Table 1

Ganetespib is more potent than 17-AAG in SCLC cell lines.

Cell line	IC50 (Ganetespib) nM	IC50 (17-AAG) nM	Fold	P value
H82	30.27	3650	120.58	<0.0001
GLC4	20.47	40.6	1.98	0.0007
H69	83.36	5800	117.08	0.0004
H128	69.55	17	0.24	0.0115
H146	28.51	1465	51.39	0.0004
H187	24.99	163,800	6554.52	0.0013
H526	21.64	2460	113.68	0.0023
N592	14.12	18.5	1.31	0.1903
H620	32.67	2455	75.15	0.0022
H792	45.07	126	2.79	0.0013
H1173	12.62	338	26.78	0.0001
AC3	25.90	10,840	418.83	<0.0001
Mean IC50	30.89	15971	193.30	<0.0001*

*One-way ANOVA

Table 2

RPPA profiling of cancer-associated proteins

	24 hrs					48 hrs				
	No Txt	**DOXO 40nM**	**GANE 30nM**	**COMB**	**p value**	**No Txt**	**DOXO 40nM**	**GANE 30nM**	**COMB**	**p value**
4EBP1_S65	1.0					1.0		3.3	2.5	0.0036
CyclinB1	1.0	3.1	1.6	2.3	0.0001	1.0	3.3		2.8	0.0006
FADD_S194	1.0	1.4	1.3	1.5	0.0094	1.0	1.3	1.3	1.5	0.0011
p90RSK_S380	1.0	0.6	0.5	0.4	0.0056	1.0	0.6	0.5	0.6	0.0121
Pyk2_Y402	1.0	0.7	0.7	0.7	0.011	1.0				
cPLA2_S505	1.0					1.0		1.4	1.5	0.0173
PDK1_S217	1.0			0.4	0.0011	1.0	1.4		1.3	0.0316
Heme-Oxygenase-1	1.0			1.3	0.0318	1.0				
SAPK_JNK_T183_Y185	1.0					1.0		0.7	0.6	0.0274
PRK1_T774_PRK2_T816	1.0		0.6	0.6	0.003	1.0		0.7	0.7	0.0113
AMPKa1_S485	1.0					1.0		0.5	0.4	0.0133
Cu_Zn_SOD	1.0					1.0		1.3	1.4	0.0045
clPARP	1.0					1.0			2.0	0.0428
CateninBeta_T41_S45	1.0			0.6	0.0342	1.0				
Alk Y1604	1.0		0.7		0.0407	1.0				
p70S6_S371	1.0	1.4			0.0068	1.0		0.7	0.7	0.0049
ATP Cytr Lyase S454	1.0	0.5	0.4	0.4	0.0336	1.0	0.5	0.4	0.4	0.0303

Values are the mean ratios derived from mean values of each treatment groups divided by mean values of the untreated control groups. Only ratios of ≤ 0.7 or ≥ 1.3 with p values < 0.05 (One-way ANOVA with Dunnett's Multiple Comparison Test) were considered significant and shown. Empty cells indicate no change in the ratio of the analysed proteins. No Txt, no treatment; Doxo, doxorubicin; Gane, ganetespib; Comb, 40nM doxorubicin + 30 nM ganetespib combination.